
This is an electronic reprint of the original article.
This reprint may differ from the original in pagination and typographic detail.

Ahadian, Hamidreza; Ceccherini, Sara; Sharifi Zamani, Elaheh; Phiri, Josphat; Maloney, Thaddeus

Production of low-density and high-strength paperboards by controlled micro-nano fibrillation of fibers

Published in:
Journal of Materials Science

DOI:
[10.1007/s10853-023-09097-9](https://doi.org/10.1007/s10853-023-09097-9)

Published: 01/11/2023

Document Version
Publisher's PDF, also known as Version of record

Published under the following license:
CC BY

Please cite the original version:
Ahadian, H., Ceccherini, S., Sharifi Zamani, E., Phiri, J., & Maloney, T. (2023). Production of low-density and high-strength paperboards by controlled micro-nano fibrillation of fibers. *Journal of Materials Science*, 58(44), 17126–17137. <https://doi.org/10.1007/s10853-023-09097-9>

This material is protected by copyright and other intellectual property rights, and duplication or sale of all or part of any of the repository collections is not permitted, except that material may be duplicated by you for your research use or educational purposes in electronic or print form. You must obtain permission for any other use. Electronic or print copies may not be offered, whether for sale or otherwise to anyone who is not an authorised user.



Production of low-density and high-strength paperboards by controlled micro-nano fibrillation of fibers

Hamidreza Ahadian^{1,2,*} , Sara Ceccherini¹, Elaheh Sharifi Zamani¹, Josphat Phiri¹, and Thaddeus Maloney^{1,*}

¹ Department of Bioproducts and Biosystems, School of Chemical Engineering, Aalto University, Espoo, Finland

² Biomass Processing and Products, VTT Technical Research Centre of Finland Ltd, Espoo, Finland

Received: 10 July 2023

Accepted: 26 October 2023

Published online:

19 November 2023

© The Author(s), 2023

ABSTRACT

One of the critical challenges in the fiber-based packaging industry is to produce low-density paperboards with high functionality and attractive cost structure. In this study, we examine how control of the hierarchical fiber swelling can be used to enhance bonding and generate a low-density fiber network with excellent strength properties. Here, the osmotic pressure inside the cell wall is increased by adding phosphate groups with a deep eutectic solvent (DES) functional drying method. Together with mechanical refining, this process causes the fibril aggregates to split and swell up massively. This effect was measured by a novel thermoporosimetry analysis method. The treated fibers have enhanced external fibrillation, fibrillar fines and bonding potential. When mixed with relatively stiff, unrefined fibers, a well-bonded sheet with lower density than a conventionally refined reference sheet was achieved. The results suggest that pulp fibers can be “nanoengineered” to enhance performance without the complications of producing and adding nanocellulose.

Introduction

In fiber-based packaging industry, having a cellulosic furnish that provides certain strength properties while maintaining cost and bulk has always been a critical issue. Bulk of a cellulose sheet matters because it can affect end product stiffness. Mechanical refining is a conventional method to enhance bonding within a paper. Refining fibrillates fibers, increases surface area

and thus increases inter-fiber bonding. However, refining typically results in slower dewatering rates during the paper-forming process and a denser final product [1–4]. Wet-end addition of micro-nanofibrillated cellulose (MNFC) is another way that has been studied in the last decade to increase bonding within a paper. Though MNFC addition to the papermaking furnishes increases paper strength, it also tends to cause production problems like slow dewatering rate and high

Handling Editor: Gregory Rutledge.

Address correspondence to E-mail: hamidreza.ahadian@vtt.fi; thaddeus.maloney@aalto.fi

shrinkage due to micro-nanodimension of the fibrils [5–9]. Therefore, it is necessary to find ways to increase the bonding capacity of the fibers while avoiding generating excess fines and fiber fragments, slowing down the dewatering rate and losing bulk of the sheets. This can possibly be achieved by chemical pretreatments of fibers to increase swelling and facilitate mechanical defibrillation [10–14].

Introducing charged groups onto pulp fibers through a chemical modification is one way to enhance delamination of fiber walls. This approach increases osmotic pressure and causes the cell wall to swell. Increased swelling results in lower energy consumption for mechanical fibrillation of fibers [12, 15–17]. One of the most well-known chemical pretreatments is the TEMPO-mediated oxidation of cellulose fibers that increases surface charge by introducing carboxylic acid groups to C-6 position [18, 19]. Concentrated sulfuric acid hydrolysis is another technique that partially dissolves the amorphous regions in cellulose and introduces anionic sulfate groups [19–21]. Other chemistries have also been exploring the increase of osmotic swelling and the potential for interfiber bonding by introducing anionic or cationic groups onto the cellulose backbone [11, 17, 22–29].

In this study, phosphate ester groups are introduced into the cell wall by a functional drying process involving a deep eutectic solvent (DES) mixture of urea and diammonium phosphate (DAP). Fibers are impregnated with the salt solution and then dried at high temperature. The salt prevents the usual hornification in drying by sterically preventing interfibrillar bonding. At sufficient temperature, the esterification reaction introduces phosphate acid groups which dissociate and promote swelling of the fiber when changed to the sodium form. Similar mixture of DAP/urea but in different dosages and settings than current research has been used by Noguchi et al. and Ghanadpour et al. [25, 26]. In this research, preparing DES mixture at higher consistencies helps minimizing curing time and energy. In a recent publication we have found that this approach can dramatically increase the fibril aggregate swelling when a threshold charge is reached [30]. This strongly increases the bonding potential of the fibers. Previous researchers have combined similar chemical treatments with applying high shear mechanical forces such as high-pressure homogenization, microfluidization, high-intensity ultrasonication, to produce and isolate the nanofibers [19, 23, 31]. However, we could not find any previous

research using DESs prior to conventional mechanical refining just to improve fiber fibrillation and not produce nanocellulose.

In the present study, we will examine DES/functional drying in combination with mechanical refining in order to enhance macrofibril deaggregation and bonding potential. We examine the use of the modified fibers in combination with low swelling unrefined pulp fibers to produce a low-density, high-strength network structure. In addition, the dewatering properties of the modified fiber furnish compared to conventional refining are examined.

Materials and methods

Phosphorylation

A never-dried, unbleached softwood Kraft pulp (UBSK) was provided by a Finnish pulp mill. Reagent grade diammonium phosphate (DAP), urea and sodium carbonate were used.

The composition for phosphorylation was: 100 g_{dry} UBSK at 25% solids content, 97 g urea, 53 g DAP. The pulp and salts were mixed for 3 h and then cured in an open container inside a ventilation hood for 30 min at 180 °C. The pulp was washed after curing until conductivity was less than 20 μS cm⁻¹. Then, the acid groups were changed to the sodium form by washing the pulp with 0,01 M HCl, DI water, Na₂CO₃ (0.02 M) and more water until the conductivity was under 20 uS cm⁻¹. The reference pulp was also adjusted to the sodium form. The samples were kept in the refrigerator at around 12% wt consistency for later usage. Furnish preparation and measurements were performed at room temperature. Deionized water was used for all experiments.

Refining and sheet making

30g_{dry} of reference and phosphorylated pulp was refined in a PFI mill (according to ISO 5264:2) at 10% solids content for 100, 250, 500, 750, 1 k, 2 k, 4 k, 7 k, 10 k revolutions. In the following, the phosphorylated pulp is called P-UBSK; the refined pulp is called R-UBSK, and the refined phosphorylated pulp is called RP-UBSK.

The two groups of handsheet with a target grammage of 80 gsm were made. The first group is made of R-UBSK pulp refined at 0, 500, 750, 1 k, 2 k and 4 k PFI

revolutions. The second group is made of unrefined UBSK pulp containing 5, 10, 15, 20 and 25% RP-UBSK which has been refined 10 k revolutions. All the hand-sheets were made according to TAPPI-T205 using a Lorentzen & Wettre FI 101 sheet mold. Sheets were pressed between three blotting papers at 4.2 bar for 4 min.

Material characterization

The water retention value (WRV) is a centrifuge test used to measure water in the cell wall. Samples were measured at $3000 \times g$ for 15 min according to SCAN-C 102 XE. The fiber morphology, including fiber length, fines content and fibrillation, was measured with a Valmet Fiber Image Analyzer FS 5. This method incorporates fiber imaging and image processing technologies. The length measuring range and accuracy is (0.01–10.00 mm). Fibrillation is calculated according to projection area of fibrils in relation to the entire projection area of entire object, scaled into a percentage. Two different categories of fines are defined in this method, Fines A and Fines B. Fines A are the flake-like solids shorter than 0.2 mm; fines A content is determined as a percentage of the projection area of measured particles. Fines B are lamella-shaped particles with width less than 10 μm and length over 0.2 mm. The sum length of these particles is divided by the sum length of all measured particles longer than 0.2 mm, scaled into a percentage. Reported fiber length is length-weighted average.

The acid group content was determined by alkaline titration according to SCAN-CM 65:02 in a Metrohm 712 Conductometric titrator by adding 0.1 M NaOH to the sample at a constant rate of 0.05 mL in every 30 s and measuring the electrical conductivity.

Thermoporosimetry was done in a Mettler Toledo DSC 3+. In this technique, the melting temperature depression of water confined in pores in the cell wall is used to calculate the pore size distribution (PSD) by application of the Gibbs-Tomson equation [32]. A semi-continuous method was used that measures the freezing exotherm in the temperature range -0.2 °C to -20 °C at a cooling rate of 2 °C min^{-1} . This covers the approximate mesopore range of cell wall pores (from 200 to 2 nm pore diameter, D). The nonfreezing water (NFW) was also considered in the measurement and is divided between a monolayer on the mesopore walls and water that does not freeze at all in micropores (below $D = 2$ nm). The mesoscale surface

area (SA) and SA distribution (SAD) were calculated from the PSD, assuming a cylindrical pore geometry. Temperature calibration was done with a step method with both 99.999% mercury and twice-distilled water at 0.02 °C steps. Enthalpy calibration was done with twice-distilled water.

Sheet characterization

The tensile strength of the sheets was measured using a Universal Tester Instron 4204. The test was conducted at 23 °C room temperature and 50% relative humidity at a 12 mm/second strain rate with a 100-N load cell. The sheet properties were determined according to the following standards and devices: density (ISO 534, L&W SE 250 D); air permeability (ISO 5636–3, Bendtsen, L&W SE 114); light scattering coefficient (Spectrophotometer Elrepho, L&W SE 070).

Dewatering properties

The dewatering experiments were performed in a modified Dynamic Drainage Analyser (DDA 5, Pulp-Eye, Sweden) with a 10 cm diameter, 325 mesh wire. 800 mL initial stock solution was used which was stirred, followed by a 10-s resting period before dewatering commenced. The water removal of 150 gsm sheets began with 30-s gravity dewatering followed by 30-s dewatering at 200 mbar vacuum. An ultrasonic-level sensor on top of the DDA vessel measured the furnish volume during drainage. The average dewatering rate from 800 to 100 mL is reported. A sheet collected just after vacuum period is dried in the oven to measure the final solids content gravimetrically.

Results and discussion

Fibers properties

Figure 1 shows the titration curves for the reference and phosphorylated pulp. The total acid group content, including contributions from weak and strong groups, has increased from 330 to 1130 $\mu\text{mol g}^{-1}$. This leads to a corresponding increase in the osmotic pressure inside the cell wall. Therefore, the WRV increases from 1.7 to 2.3 mL g^{-1} after the phosphorylation. The true magnitude of this change becomes evident after the pulps are refined. In Fig. 2, the WRV increases from 1.7 to 2.2 mL g^{-1} after 10 k revs of refining for

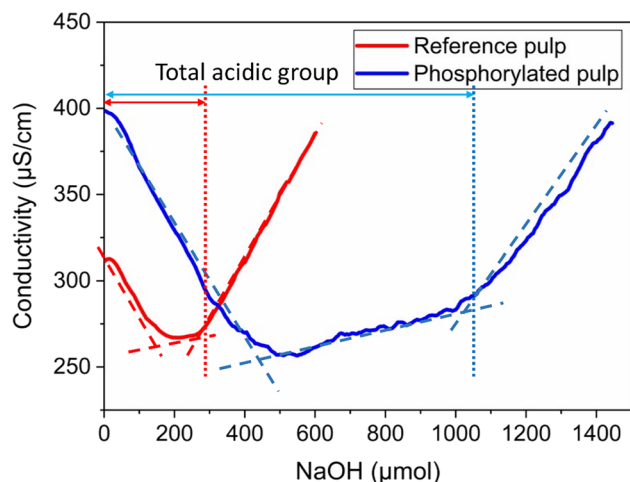


Figure 1 Conductometric titration curves of UBSK and P-UBSK.

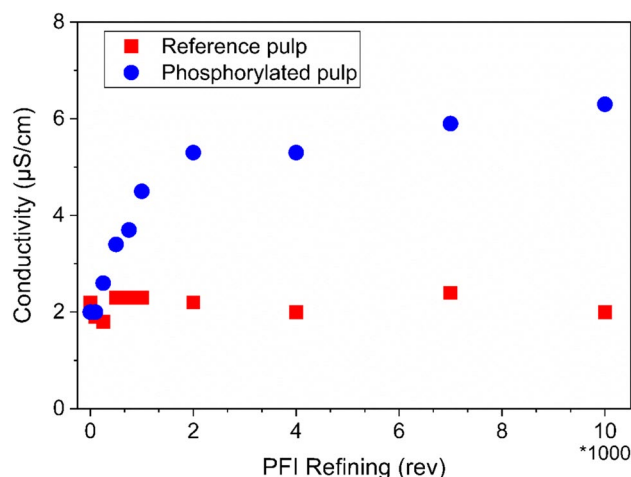


Figure 3 Conductivity of UBSK pulp and P-UBSK pulps as a function of PFI refining revolutions.

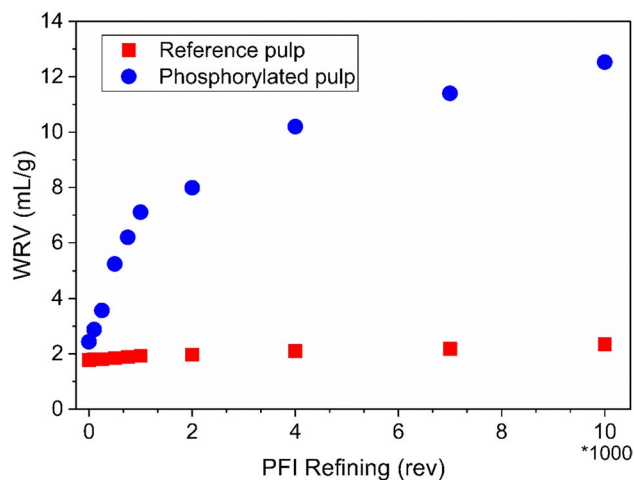


Figure 2 Water retention value of UBSK pulp and P-UBSK pulps as a function of PFI refining revolutions.

the unmodified pulp. The P-UBSK sample increases to around 12 mL g^{-1} over the same refining range. The increased osmotic pressure augments the rupture of internal cell wall bonds when the pulp is refined. As a result, internal fibrillation is enhanced, and the bonding potential is magnified. Figure 3 shows that salts which are trapped in the cell wall during the functional drying are released when the fiber is refined. Cell wall pores open up, allowing the diffusion of salts to the exterior solution.

In this study, the fibers were modified by a combination of phosphorylation and mechanical refining. The phosphorylation adds charge to the fibril

surfaces and increases osmotic pressure and swelling. Mechanical refining ruptures cell wall bonds and lowers the modulus, leading to increased cell wall swelling. The structural effects of refining, either with or without phosphorylation, are shown in Fig. 4 and Table 1.

When the reference pulp is refined, there is a modest increase in the mesoscale surface area, mesopore and macropore volume. Phosphorylation increases the mesoscale surface area and pore volume compared to the reference. Upon the refining, the mesoscale surface area further increases to a value of nearly $1800 \text{ m}^2 \text{ g}^{-1}$. We interpret this increase as a deaggregation of macrofibrils. Likewise, refining, phosphorylation and especially the combination of the two increase the mesopore and macropore volumes.

In earlier studies, we have found that refining predominantly causes an expansion of the cell wall lamellae (increasing macropores) and has a relatively little small impact on mesopore volumes. In other words, refining of unmodified chemical pulp does not greatly split the macrofibrils. In this study, the phosphorylation has a pronounced effect on the mesopore volume. Likewise, the surface area plots in Fig. 4 show a dramatic change after phosphorylation. The shape of the curves shifts from a nearly monomodal distribution to a clearly bimodal. We believe this structural change is related to the deaggregation of fibril aggregates formed by the hornification of the cell wall when the fibers were formed in chemical

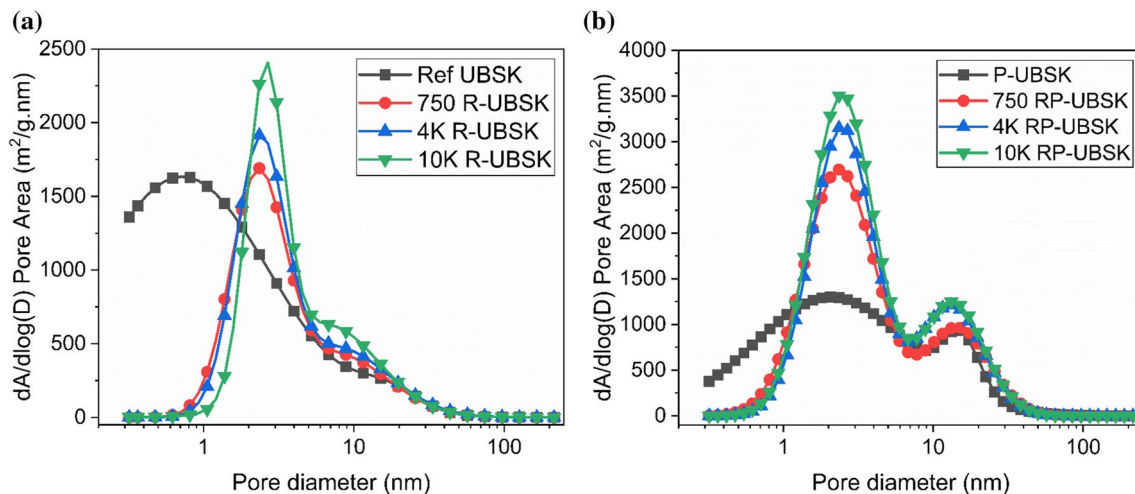


Figure 4 Derivative surface area of refined pulp calculated from DSC thermoporosimetry analysis, **a** unphosphorylated pulps, **b** phosphorylated pulps.

Table 1 The mesoscale surface area and pore volume, WRV and macropore volume of the refined pulps calculated from DSC thermoporosimetry analysis

Samples	Mesopore surface area ($\text{m}^2 \text{g}^{-1}$)	Mesopore volume (mL g^{-1})	WRV (mL g^{-1})	Macropore volume (mL g^{-1})
UBSK	557	1.23	1.78	0.55
750 rev R-UBSK	720	1.21	1.89	0.68
4 k rev R-UBSK	804	1.34	2.11	0.77
10 k rev R-UBSK	957	1.43	2.35	0.92
P-UBSK	1000	2.21	2.44	0.23
750 rev RP-UBSK	1390	2.82	6.20	3.38
4 k rev RP-UBSK	1620	3.11	10.20	7.09
10 k rev RP-UBSK	1760	3.34	12.53	9.19

pulping. The swelling of the hierarchical structures within the cell wall is expected to have significant consequences for fiber flexibility, bonding, consolidation and dewatering. [32–37]

Figure 5 shows the external fibrillation, fines content and fiber length of the pulps as a function of refining amount. It is most notable that the phosphorylation allows for the enhanced development of external fibrillation (Fig. 5a) and increases number of fibrillar fines while having limited impact on flake-like fines generation (Fig. 5b, d). The flake-like fines are largely fragments of the outer cell wall and ray cells and thus are not greatly impacted by the phosphorylation procedure. However, the phosphorylation helps increase fibril split and deaggregation, thus increasing both external fibrillation and fibrillar fines generation. Fibrillar fines are well known to have a significant impact on fiber bonding and strength properties.

Figure 6 shows the microscopic images of the UBSW and P-UBSW fibers before and after refining. The P-UBSW fibers are seen to balloon even before refining. In regions where the outer cell wall is weak or entirely missing, the increased osmotic pressure from phosphorylation causes the cell wall to balloon between collars. However, many of the fibers do not show ballooning at all. The enhanced swelling appears to be quite heterogeneous; concentrated on certain fibers and certain parts of the cell wall [37–39].

Sheet properties

The two different groups of sheets were characterized to investigate the potential of highly swollen pulp in paper and board making. The first group (shown by red squares in all figures) of handsheets is made of 100% UBSK pulp refined to different extents. The

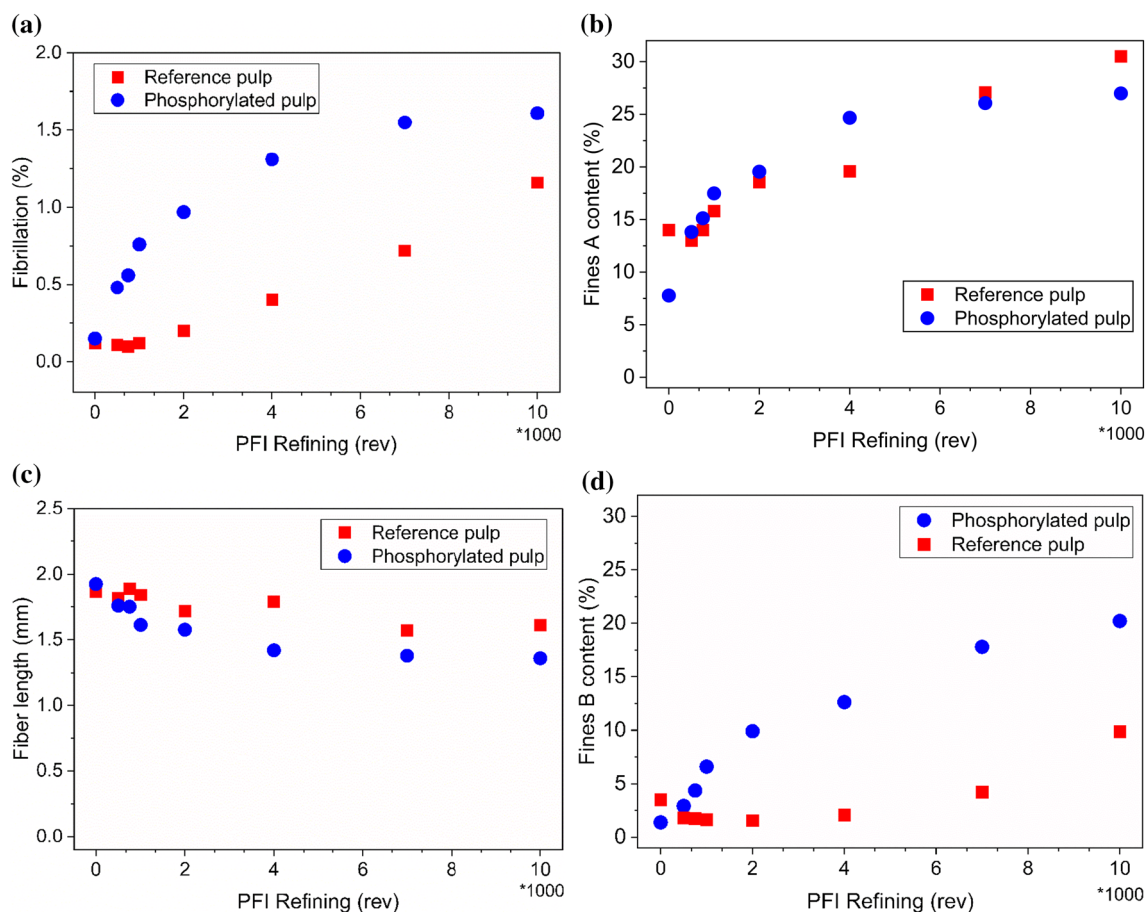


Figure 5 The physical properties of reference and phosphorylated fibers as a function of PFI refining revolutions, **a** fibrillation, **b** fines A content, **c** fiber length, **d** fines B content.

second group (shown by blue circles in all figures) is a blend of UBSK and 10 k rev refined RP-UBSK. Figure 7 shows the density of both sheet series.

The density of UBSK sheets increases from 0.5 to 0.63 g cm⁻³ after 4 k rev of refining. While necessary to increase bond area, this is negative for producing light weight structures, such as low-density folding boxboard. An alternative approach is to add the highly swollen RP-UBSK to a network of unrefined UBSK. The unrefined UBSK has a stiff enough fiber to prevent the structure from densifying in consolidation. The RP-UBSK has high surface area and swelling and can bond the structure together. Figure 7 shows that composite sheets of UBSK/RP-UBSK have a lower density than the refined UBSK sheets alone. Furthermore, the blend has a more favorable density/modulus relationship as shown in Fig. 8. The elastic forces within a network of relatively stiff reference fibers and flexible modified fibers are sufficient to re-expand and regain

some of its bulk after wet pressing. At any modulus, the blend has a lower density than the conventional refining case [2, 3, 40, 41].

Few researchers have evaluated minimized refining and compensation with surface modification of pulp fibers. Rice et al. utilized nanofibrillated cellulose pretreated with cationic starch as a bonding system in handsheets. Pretreated NFC was particularly effective in increasing the tensile strength and stiffness of low-refined sheets. Their strategy allowed improved tensile strength at a lower apparent density (high bulk) of the handsheets which authors suggest using it as a substitute for mechanical refining of pulp fibers for specific paper grades [2]. Pettersson et al. used starch and CMC for CTMP fibers surface treatment. They reduced refining energy and produced strong and bulky paperboards [42]. Jan Eric berg et al. optimized process conditions in low-consistency (LC) refining, i.e., LC refiner filling patterns, in order to

Figure 6 Optical microscopy images of fiber, **a** UBSK, **b** P-UBSK, **c** 10 k rev refined UBSK, **d** 10 k rev refined P-UBSK.

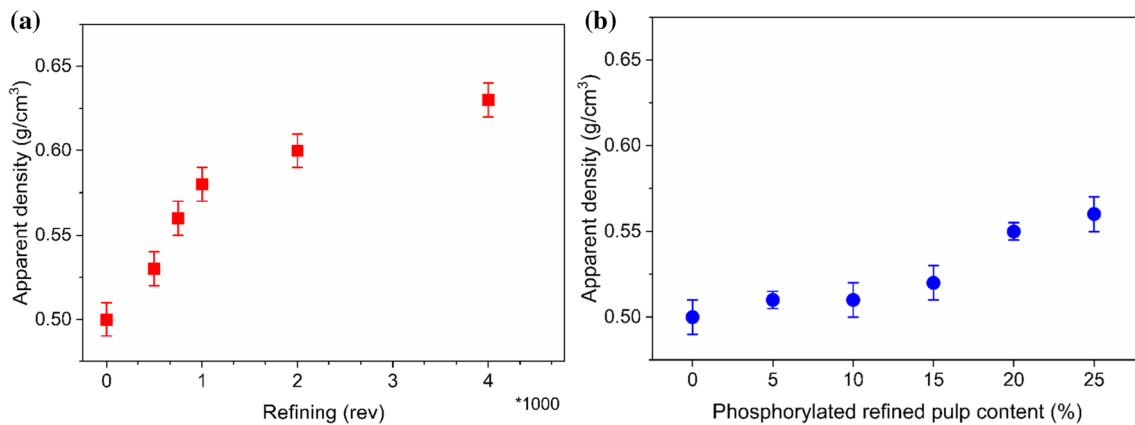
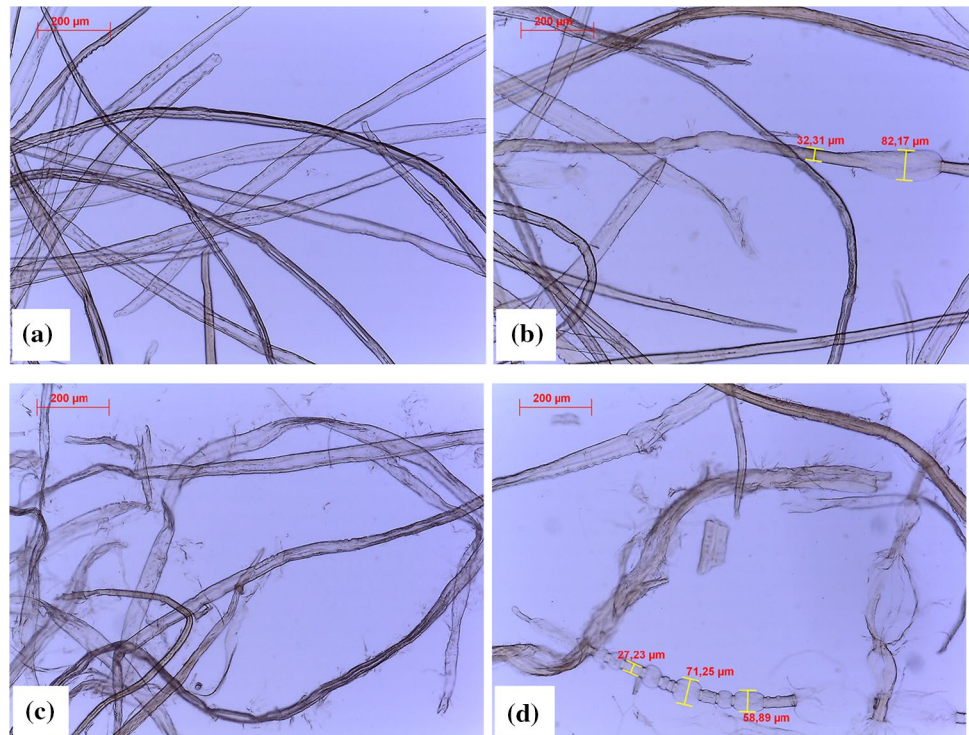


Figure 7 The density of sheets from **a** R-UBSK as a function of PFI refining revolutions, **b** UBSK as a function of 10 k rev RP-UBSK content.

produce fibrillar fines and improve the separation of fibers from each other while preserving the natural fiber morphology as much as possible. A fine filling pattern resulted in sheets with higher tensile index at maintained bulk compared to a standard filling pattern [43].

The structure of interfiber bonds is influenced by refining or the addition of phosphorylated pulp. Light scattering coefficient can be used as an indicator of interfiber bonding area, with lower light scattering,

indicating higher relative bond area. In this experiment, the light scattering decreased either by increased refining or addition of phosphorylated pulp (Fig. 9a). This means that both approaches increase fiber contact. Besides, the sheets containing 10 k rev RP-UBSK have a higher light scattering coefficient in a certain tensile strength which suggest that the phosphorylated pulps give a higher specific bond strength than the conventional refining (Fig. 9a) [41, 44]. Furthermore, the sheets containing 10 k RP-UBSK are less permeable

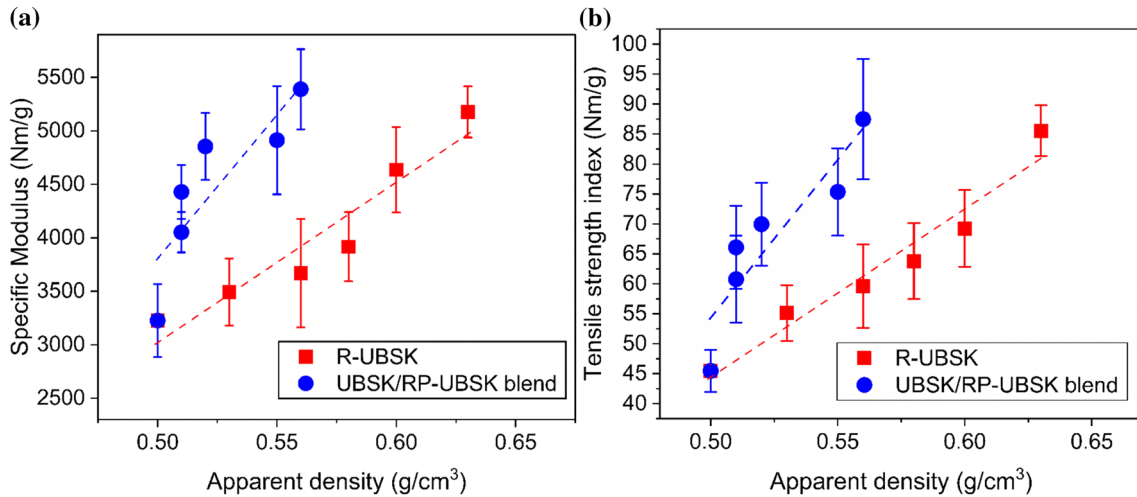


Figure 8 The mechanical strength properties of sheets from R-UBSK refined at different PFI revolutions and from UBSK containing different contents of 10 k rev RP-UBSK, **a** specific modulus, **b** tensile strength index.

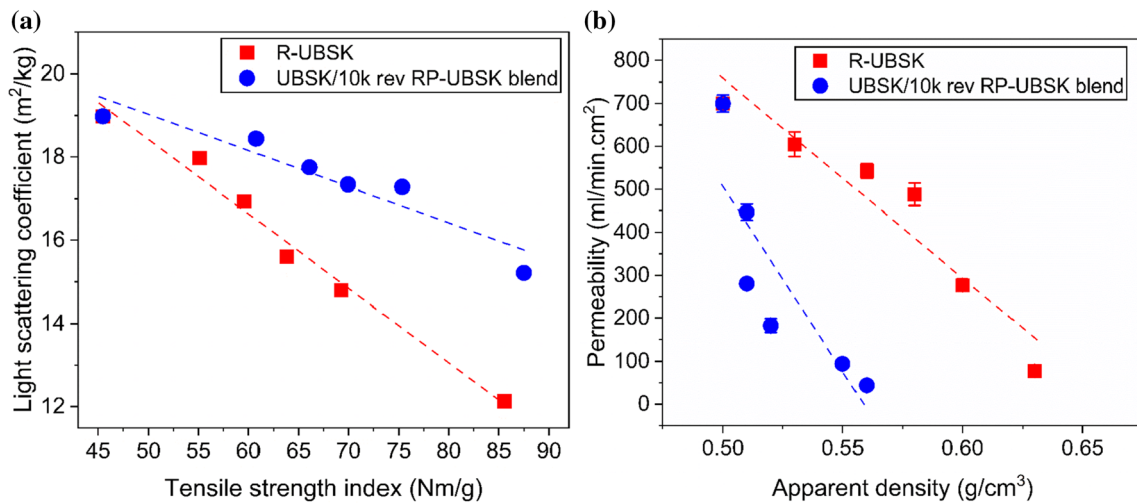


Figure 9 The properties of sheets from R-UBSK refined at different PFI revolutions and from UBSK containing different contents of 10 k rev RP-UBSK **a** light scattering, **b** air permeability.

than R-UBSK sheets, while they are bulkier and more porous (Fig. 9b). Highly fibrillated fibers and fibrillar fines fill voids between unrefined fibers, creating a low permeability closed sheet. This is consistent with fibrillation and Fines B content in Fig. 5d.

In Fig. 10a, the SEM images of the UBSK sheets show intact, unfibrillated fibers. In the sheet made of R-UBSK, only partial surface fibrillation and small interfiber films are visible. For the sheet containing phosphorylated pulp, the surface is highly closed by a film. Film forming is due to presence of highly fibrillated fibers and fibrillar fines. There is a covered area by a film (red arrows) that we believe it is one

relatively long microfibrillated fiber rather than individual bonded fibrils. Typically, a sealed wire-side surface is the result of fines enrichment. This is well known to have a serious negative impact on sheet dewatering. In this case, it is actually the microfibrillated fibers which contribute to sheet sealing. At the 25% concentration, used in this experiment, there is a high enough concentration of these highly fibrillated fibers to seal the wire side surface effectively.

It is important that new furnish solutions not only lead to better functionality but can be manufactured efficiently. Thus, dewatering is a relevant property. In this case, the two furnish solutions are compared

Figure 10 SEM images of the sheets (wire-side) made from a) reference UBSK, **b** 4 k rev R-UBSK, **c** blend of UBSK and 25% 10 k rev RP-UBSK.

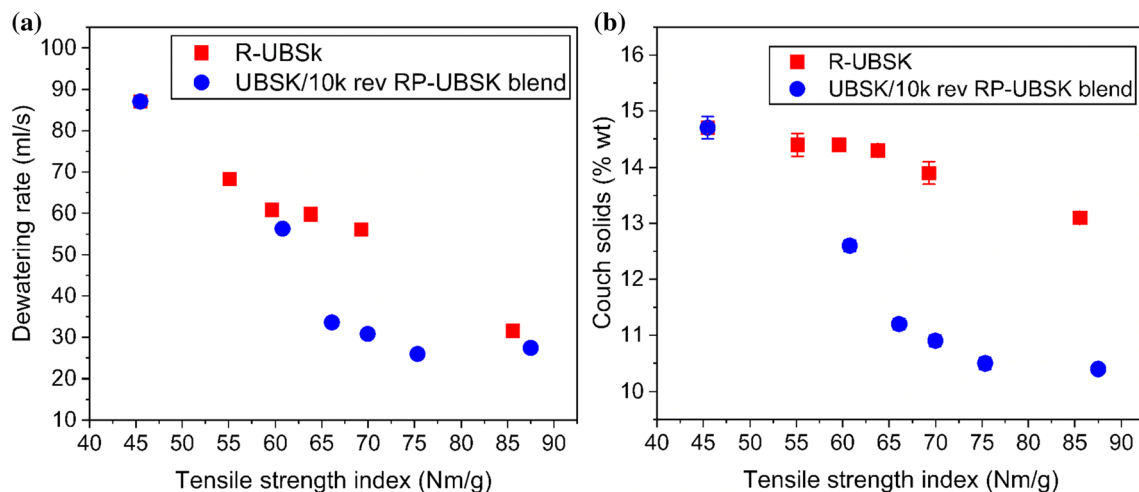
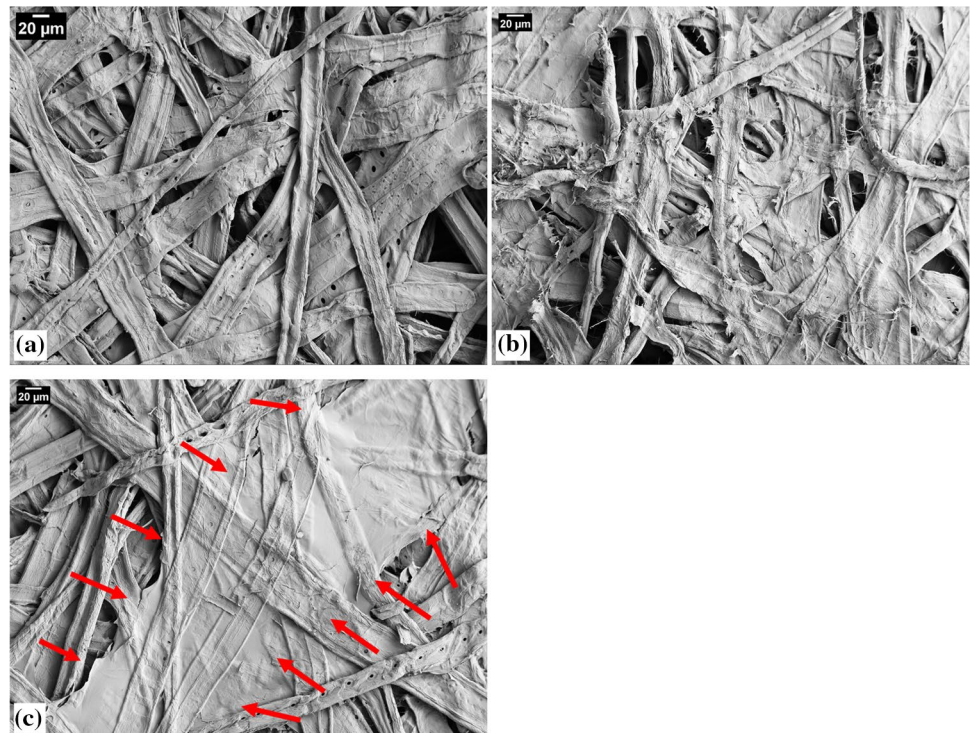


Figure 11 Dewatering properties of the sheets from R-UBSK refined at different PFI revolution and from UBSK containing different contents of 10 k rev RP-UBSK **a** dewatering rate, **b** couch solids.

at equal tensile strength. This is shown in Fig. 11 for dewatering rate and couch solids. Both the water removal rate and the solids content following vacuum dewatering (couch solids) are relevant for overall water removal efficiency and paper machine speed.

The dewatering rate is higher for the conventional refining over most of the range when compared on a tensile strength basis. We believe this is due to the

effect of the phosphorylated pulp on permeability and sheet sealing discussed above. It appears that the plugging of interfiber pores manifests itself already in the water-saturated state where dewatering rate is relevant.

The couch solids relate to the swelling and capillarity of the web after a specified vacuum period. Couch solids are a function of both the compression of the web under

vacuum and the displacement of water from interfiber capillaries. Unrefined pulp would normally provide a permeable capillary system that is easy to dewater by vacuum. However, when the unrefined fibers are mixed with refined phosphorylated pulp, with a WRV around 12 mL g^{-1} , the interstitial pores are effectively filled with high swelling microfibrils that effectively retain water. So, the couch solids of the blended pulp are very low compared to conventional refining. These results indicate that further optimization of variables will be required to utilize composite pulp systems. Although the strength/density relationship of the phosphorylated/unrefined pulp blends is very promising, the low dewatering rate is a serious drawback.

Conclusion

In this work, a deep eutectic solvent (DES) functional drying method was utilized to enhance hierarchical fiber swelling. As a result, we could facilitate cell wall delamination and deaggregation of cellulose fibrils during mechanical fibrillation. It was shown that mesoscale swelling and surface area increased greatly through a combination of phosphorylation and mechanical fibrillation. This resulted from increased osmotic pressure within the cell wall in combination with shear and cyclic compression in refining. The phosphorylated pulp was found to swell and fibrillate in refining, but not degrade to flake-like fines any faster than unmodified pulp. Adding this highly fibrillated swollen pulp to an unrefined fiber furnish made it possible to produce a family of sheets with higher strength/density ratio compared to conventional refining. The pretreated pulp was found to have lower sheet permeability and film form on the exit layer. Dewatering analysis showed that the phosphorylated/unrefined pulp blend had a lower dewatering rate and couch solids than the conventionally refined reference. Though the composite pulp strategy leads to less refining need of the main fiber furnish and promising sheet properties, further optimizations are needed to decrease the negative impact on dewatering behavior for commercial applications.

Acknowledgements

This research was funded by Jane and Aatos Erkkö Foundation (3269-7422e). This work made use of Aalto University Bioeconomy Facilities. The SEM imaging

was conducted at Aalto University Nanomicroscopy Centre (Aalto-NMC).

Authors contributions

H.A helped in conceptualization, methodology, investigation, analysis, writing—original draft; S.C assisted with methodology of phosphorylation process; E.S assisted with investigations; J.P assisted with analysis of thermoporosimetry data; T.M was involved in conceptualization, supervision, writing—review & editing.

Funding

Open Access funding provided by Technical Research Centre of Finland.

Data availability

All data and materials are included within the manuscript.

Declarations

Conflict of interest The authors report no conflicts of interest. The authors alone are responsible for the content and writing of the paper.

Open Access This article is licensed under a Creative Commons Attribution 4.0 International License, which permits use, sharing, adaptation, distribution and reproduction in any medium or format, as long as you give appropriate credit to the original author(s) and the source, provide a link to the Creative Commons licence, and indicate if changes were made. The images or other third party material in this article are included in the article's Creative Commons licence, unless indicated otherwise in a credit line to the material. If material is not included in the article's Creative Commons licence and your intended use is not permitted by statutory regulation or exceeds the permitted use, you will need to obtain permission directly from the copyright holder. To view a copy of

this licence, visit <http://creativecommons.org/licenses/by/4.0/>.

References

- [1] Lindström T, Wågberg L, Larsson T (2005) On the nature of joint strength in paper-A review of dry and wet strength resins used in paper manufacturing. In: *Advances in paper science and technology, Trans of the XIIIth Fund Res Symp Cambridge, 2005*, (SJ I'Anson, ed), pp 457–562. FRC, Manchester, 2018. <https://doi.org/10.15376/frc.2005.1.457>
- [2] Rice MC, Pal L, Gonzalez R, Hubbe MA (2018) Wet-end addition of nanofibrillated cellulose pretreated with cationic starch to achieve paper strength with less refining and higher bulk. *Tappi J* 17:395–403. <https://doi.org/10.32964/tj17.07.395>
- [3] Hubbe MA (2019) Nanocellulose, cationic starch and paper strength. *Appita J* 72(2):82–94
- [4] Koponen A, Haavisto S, Liukkonen J, Salmela J (2016) The flow resistance of fiber sheet during initial dewatering. *Drying Technol* 34:1521–1533. <https://doi.org/10.1080/07373937.2015.1132427>
- [5] Zambrano F, Starkey H, Wang Y et al (2020) Using micro- and nanofibrillated Cellulose as a means to reduce weight of paper products: a review. *BioResources* 15:4553–4590. <https://doi.org/10.15376/biores.15.2>
- [6] Ahadian H, Sharifi Zamani E, Phiri J, Maloney T (2021) Fast dewatering of high nanocellulose content papers with in-situ generated cationic micro-nano bubbles. *Drying Technol*. <https://doi.org/10.1080/07373937.2021.1942898>
- [7] Samyn P, Barhoum A, Dufresne A (2018) Review: nanoparticles and nanostructured materials in papermaking. *J Mater Sci* 53:146–184. <https://doi.org/10.1007/s10853-017-1525-4>
- [8] Eichhorn SJ, Dufresne A, Aranguren M et al (2010) Review: current international research into cellulose nanofibres and nanocomposites. *J Mater Sci* 45:1–33. <https://doi.org/10.1007/s10853-009-3874-0>
- [9] Mandlez D, Koller S, Eckhart R et al (2022) Quantifying the contribution of fines production during refining to the resulting paper strength. *Cellulose*. <https://doi.org/10.1007/s10570-022-04809-x>
- [10] Kibblewhite RP (1975) Interrelations between pulp refining treatments, fibre and pulp fines quality, and pulp freeness. *Paperi Ja Puu-Paper Timber* 57:519–526
- [11] Kokol V, Božič M, Vogrinčič R, Mathew AP (2015) Characterisation and properties of homo- and heterogeneously phosphorylated nanocellulose. *Carbohydr Polym* 125:301–313. <https://doi.org/10.1016/J.CARBPOL.2015.02.056>
- [12] Karlsson RM, Larsson PT, Pettersson T, Wågberg L (2020) Swelling of cellulose-based fibrillar and polymeric networks driven by ion-induced osmotic pressure. *Langmuir*. <https://doi.org/10.1021/acs.langmuir.0c02051>
- [13] Isogai A, Zhou Y (2019) Diverse nanocelluloses prepared from TEMPO-oxidized wood cellulose fibers: Nanonetworks, nanofibers, and nanocrystals. *Curr Opin Solid State Mater Sci* 23:101–106. <https://doi.org/10.1016/J.COSSMS.2019.01.001>
- [14] Kargupta W, Seifert R, Martinez M et al (2021) Sustainable production process of mechanically prepared nanocellulose from hardwood and softwood: A comparative investigation of refining energy consumption at laboratory and pilot scale. *Ind Crops Prod*. <https://doi.org/10.1016/J.INDCROP.2021.113868>
- [15] Aguado R, Lourenço AF, Ferreira PJT et al (2019) The relevance of the pretreatment on the chemical modification of cellulosic fibers. *Cellulose* 26:5925–5936. <https://doi.org/10.1007/S10570-019-02517-7/FIGURES/5>
- [16] Pere J, Tammelin T, Niemi P et al (2020) Production of high solid Nanocellulose by enzyme-aided fibrillation coupled with mild mechanical treatment. *Cite This ACS Sustain Chem Eng* 8:18853–18863. <https://doi.org/10.1021/acssuschemeng.0c05202>
- [17] Guccini V, Phiri J, Trifol J et al (2022) Tuning the porosity, water interaction, and redispersion of nanocellulose hydrogels by osmotic dehydration. *ACS Appl Polym Mater* 4:24–28. <https://doi.org/10.1021/acsapm.1c01430>
- [18] Isogai A (2021) Emerging Nanocellulose technologies: recent developments. *Adv Mater*. <https://doi.org/10.1002/ADMA.202000630>
- [19] Nechyporchuk O, Belgacem MN, Bras J (2016) Production of cellulose nanofibrils: A review of recent advances. *Ind Crops Prod* 93:2–25. <https://doi.org/10.1016/J.INDCROP.2016.02.016>
- [20] Tang Y, Yang H, Vignolini S (2022) Recent progress in production methods for cellulose nanocrystals: leading to more sustainable processes. *Adv Sustain Syst*. <https://doi.org/10.1002/ADSU.202100100>
- [21] Punia Bangar S, Harussani MM, Ilyas RA, et al (2022) Surface modifications of cellulose nanocrystals: Processes, properties, and applications. <https://doi.org/10.1016/j.foodhyd.2022.107689>
- [22] Ho TTT, Zimmermann T, Hauert R, Caseri W (2011) Preparation and characterization of cationic nanofibrillated cellulose from etherification and high-shear disintegration

- processes. *Cellulose* 18:1391–1406. <https://doi.org/10.1007/S10570-011-9591-2>
- [23] Illy N, Fache M, Ménard R et al (2015) Phosphorylation of bio-based compounds: the state of the art. *Polym Chem* 6:6257. <https://doi.org/10.1039/c5py00812c>
- [24] Naderi A, Lindström T, Weise CF et al (2016) Phosphorylated nanofibrillated cellulose: Production and properties. *Nord Pulp Paper Res J* 31:20–29. <https://doi.org/10.3183/NPPRJ-2016-31-01-P020-029/MACHINEREADEABLE CITATION/RIS>
- [25] Noguchi Y, Homma I, Matsubara Y (2017) Complete nanofibrillation of cellulose prepared by phosphorylation. *Cellulose* 24:1295–1305. <https://doi.org/10.1007/S10570-017-1191-3/FIGURES/11>
- [26] Ghanadpour M, Carosio F, Larsson PT, Wågberg L (2015) Phosphorylated Cellulose Nanofibrils: A Renewable Nanomaterial for the Preparation of Intrinsically Flame-Retardant Materials. *Biomacromol* 16:3399–3410. https://doi.org/10.1021/ACS.BIOMAC.5B01117/ASSET/IMAGES/LARGE/BM-2015-01117D_0012.JPEG
- [27] Rocha I, Ferraz N, Mihranyan A et al (2018) Sulfonated nanocellulose beads as potential immunosorbents. *Cellulose* 25:1899–1910. <https://doi.org/10.1007/S10570-018-1661-2/FIGURES/8>
- [28] Iwamoto S, Endo T (2015) 3 nm thick lignocellulose nano fibers obtained from esterified wood with maleic anhydride. *ACS Macro Lett* 4:80–83. https://doi.org/10.1021/MZ500787P/ASSET/IMAGES/LARGE/MZ-2014-00787P_0004.JPEG
- [29] Li S, Xiong Q, Lai X et al (2016) Molecular Modification of Polysaccharides and Resulting Bioactivities. *Compr Rev Food Sci Food Saf* 15:237–250. <https://doi.org/10.1111/1541-4337.12161>
- [30] Maloney T, Phiri J, Zitting A, et al (2023) Deaggregation of cellulose macrofibrils and its effect on bound water. *Carbohydr Polym* 121166. <https://doi.org/10.1016/J.CARPOL.2023.121166>
- [31] Almeida RO, Maloney TC, Gamelas JAF (2023) Production of functionalized nanocelluloses from different sources using deep eutectic solvents and their applications. *Ind Crops Prod* 199:. <https://doi.org/10.1016/J.INDCROP.2023.116583>
- [32] Maloney TC (2015) Thermoporosimetry of hard (silica) and soft (cellulosic) materials by isothermal step melting. *J Therm Anal Calorim* 121:7–17. <https://doi.org/10.1007/s10973-015-4592-2>
- [33] Nopens M, Sazama U, König S, et al (2020) Determination of mesopores in the wood cell wall at dry and wet state. *Scientific Reports* 2020 10:1 10:1–11. <https://doi.org/10.1038/s41598-020-65066-1>
- [34] Aarne N, Kontturi E, Laine J (2012) Influence of adsorbed polyelectrolytes on pore size distribution of a water-swollen biomaterial. *Soft Matter* 8:4740–4749. <https://doi.org/10.1039/C2SM07268H>
- [35] Paajanen A, Ceccherini S, Maloney T, Ketoja JA (2019) Chirality and bound water in the hierarchical cellulose structure. *Cellulose* 26:5877–5892. <https://doi.org/10.1007/S10570-019-02525-7/TABLES/3>
- [36] Maloney T, Paulapuro H (1999) The formation of pores in the cell wall. *J Pulp Pap Sci* 25:430–436
- [37] Parviainen H, Parviainen A, Virtanen T et al (2014) Dissolution enthalpies of cellulose in ionic liquids. *Carbohydr Polym* 113:67–76. <https://doi.org/10.1016/J.CARPOL.2014.07.001>
- [38] Kekäläinen K, Liimatainen H, Illikainen M et al (2014) The role of hornification in the disintegration behaviour of TEMPO-oxidized bleached hardwood fibres in a high-shear homogenizer. *Cellulose* 21:1163–1174. <https://doi.org/10.1007/S10570-014-0210-X/FIGURES/7>
- [39] Cuissinat C, Navard P (2006) Swelling and Dissolution of Cellulose Part 1: Free Floating Cotton and Wood Fibres in N-Methylmorpholine-N-oxide–Water Mixtures. *Macromol Symp* 244:1–18. <https://doi.org/10.1002/MASY.200651201>
- [40] González I, Alcalà M, Chinga-Carrasco G, et al (2014) From paper to nanopaper: Evolution of mechanical and physical properties. *Cellulose* 21:2599–2609. <https://doi.org/10.1007/s10570-014-0341-0>
- [41] Motamedian HR, Halilovic AE, Kulachenko A (2019) Mechanisms of strength and stiffness improvement of paper after PFI refining with a focus on the effect of fines. *Cellulose*. <https://doi.org/10.1007/s10570-019-02349-5>
- [42] Pettersson G, Höglund H, Norgren S et al (2015) Strong and bulky paperboard sheets from surface modified CTMP, manufactured at low energy. *Nord Pulp Paper Res J*. <https://doi.org/10.3183/npprj-2015-30-02-p319-325>
- [43] Berg JE, Hellstadius B, Lundfors M, Engstrand P (2021) Low-consistency refining of CTMP targeting high strength and bulk: Effect of filling pattern and trial scale. *Nord Pulp Paper Res J*. <https://doi.org/10.1515/npprj-2020-0061>
- [44] Ketola AE, Strand A, Sundberg A et al (2018) Effect of micro- and Nanofibrillated cellulose on the drying shrinkage, extensibility, and strength of fibre networks. *BioResources* 13:5319–5342. <https://doi.org/10.15376/biores.13.3.5319-5342>

Publisher's Note Springer Nature remains neutral with regard to jurisdictional claims in published maps and institutional affiliations.